Hindawi
Complexity
Volume 2017, Article ID 3273408, 10 pages
https://doi.org/10.1155/2017/3273408

WILEY | Hindawi

Research Article

Dynamic Analysis and Circuit Design of a Novel Hyperchaotic System with Fractional-Order Terms

Abir Lassoued and Olfa Boubaker

National Institute of Applied Sciences and Technology (INSAT), Centre Urbain Nord, BP 676, 1080 Tunis Cedex, Tunisia

Correspondence should be addressed to Abir Lassoued; lassoued.abir5@gmail.com

Received 28 June 2017; Revised 19 September 2017; Accepted 1 October 2017; Published 26 October 2017

Academic Editor: Dimitri Volchenkov

A novel hyperchaotic system with fractional-order (FO) terms is designed. Its highly complex dynamics are investigated in terms of equilibrium points, Lyapunov spectrum, and attractor forms. It will be shown that the proposed system exhibits larger Lyapunov exponents than related hyperchaotic systems. Finally, to enhance its potential application, a related circuit is designed by using the MultiSIM Software. Simulation results verify the effectiveness of the suggested circuit.

1. Introduction

Hyperchaos was discovered by Rössler in 1979 [1] and the first hyperchaotic circuit was implemented by Matsumoto in 1986 [2]. In these last years, hyperchaotic systems have gained the interest of the scientific community and new systems and circuits are proposed [3–8]. This great interest can be explained by the aptitude of hyperchaotic systems to generate complex dynamics characterized by more than one positive Lyapunov exponent and attractors deployed in multiple directions. In practical applications and particularly in secure communication, chaotic synchronization has been explored by using electronic circuits, namely, Duffing circuit [9], Chua circuit [10], and Rössler circuit [11]. However, for hyperchaotic circuits, many challenging problems are still pending due to their complex behaviors.

On the other hand, several researches have attempted to construct chaotic and hyperchaotic models with simple algebraic structures highly recommended for circuit design. The most famous chaotic one is the Jerk system proposed by sprott, in 1994 [12, 13], which contains simple nonlinear terms. However, it is well known that most systems contain conventional nonlinear terms like piecewise linear functions [14–17], integer order polynomials [8, 18], sine functions [19], time delayed functions [20], and switching functions [21]. In this framework, fractional-order polynomials could be used to build complex chaotic behaviors and, to the best of our knowledge, they have not been harnessed until now.

The purpose of this paper is to build a novel hyperchaotic system with more complex dynamics than those proposed by related works. Expecting that the PWNL function with FO terms gives us more complex chaotic proprieties than the piecewise linear one, this PWNL function is constructed from absolute functions and FO polynomials. To enhance the potential application of the proposed system, its related circuit is designed afterwards with MultiSIM Software.

The rest of this paper is structured as follows. In Section 2, the mathematical model of the hyperchaotic system is proposed and its basic properties are presented. In Section 3, the dynamic analysis of the novel system is investigated by pointing out its elementary characteristics such as the Lyapunov exponents, the attractor forms, and the equilibrium points. In Section 4, the oscillator circuit of the hyperchaotic system is designed afterwards.

2. Mathematical Model and Basic Properties

Let consider the mathematical model of the novel hyperchaotic system with FO terms expressed by the following differential equations:

$$\dot{x} = y,$$
$$\dot{y} = z,$$

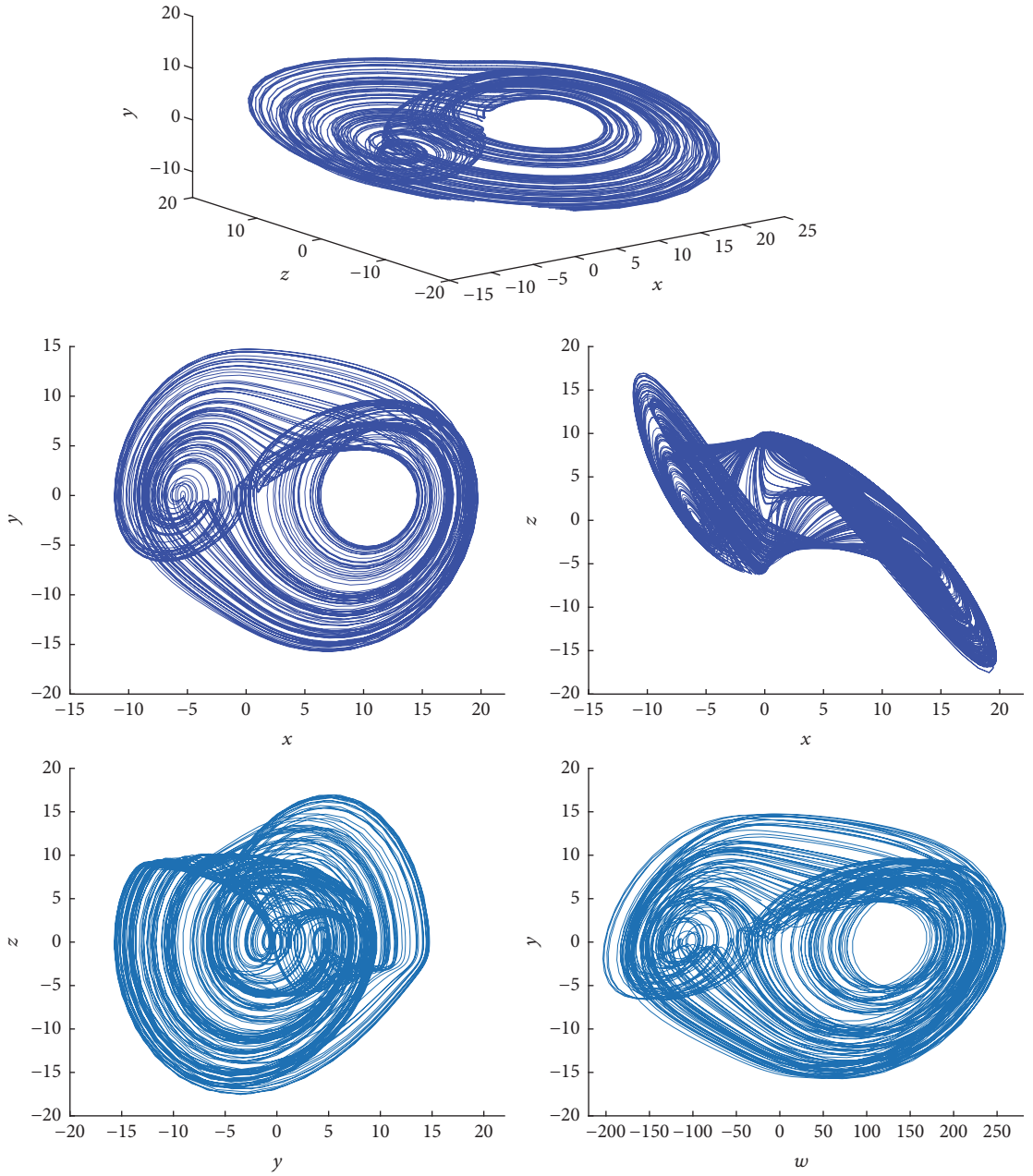

Figure 1: Projections of the attractor related to the hyperchaotic system (1) onto the spaces (x, y, z), (x, y), (x, z), (y, z), and (w, y).

$$\begin{aligned} \dot{z} &= -az - by + G(x) \\ \dot{w} &= ky - hw + G(x), \end{aligned} \tag{1}$$

with $G(x)$ being a nonlinear function defined as

$$G(x) = -cx^2 + d|x|x + m|x|^r x^{-1}, \quad 1 < r < 2, \tag{2}$$

where (a, b, c, d, h, k, m, r) are the system's parameters and (x, y, z, w) are the state variables. r is a fractional number satisfying $1 < r < 2$. Since $r \neq 1$, $|x|^r x^{-1}$ will never be an indeterminate form. The nonlinear function $G(x)$ can be written as follows:

$$G(x) = \begin{cases} (-c-d)x^2 - m(-x)^{r-1}, & \text{if } x < 0, \\ 0, & \text{if } x = 0, \\ (-c+d)x^2 + mx^{r-1}, & \text{if } x > 0. \end{cases} \tag{3}$$

System (1) can exhibit chaotic behavior if the general condition of dissipativity is satisfied such as

$$\frac{\partial \dot{x}}{\partial x} + \frac{\partial \dot{y}}{\partial y} + \frac{\partial \dot{z}}{\partial z} + \frac{\partial \dot{w}}{\partial w} = -a - h < 0. \tag{4}$$

As long as $a + h > 0$, system (1) is dissipative and it converges to an attractor. Thus, when the parameters (a, b, c, d, m, r, h, k) are equal to $(0.93, 1.11, -0.11, -0.21, 6.26, 1.32, 0.001, 14)$ and the initial condition is equal to $(1, 1, 1, 1)$, system (1) generates a strange attractor displayed in Figure 1. This attractor has

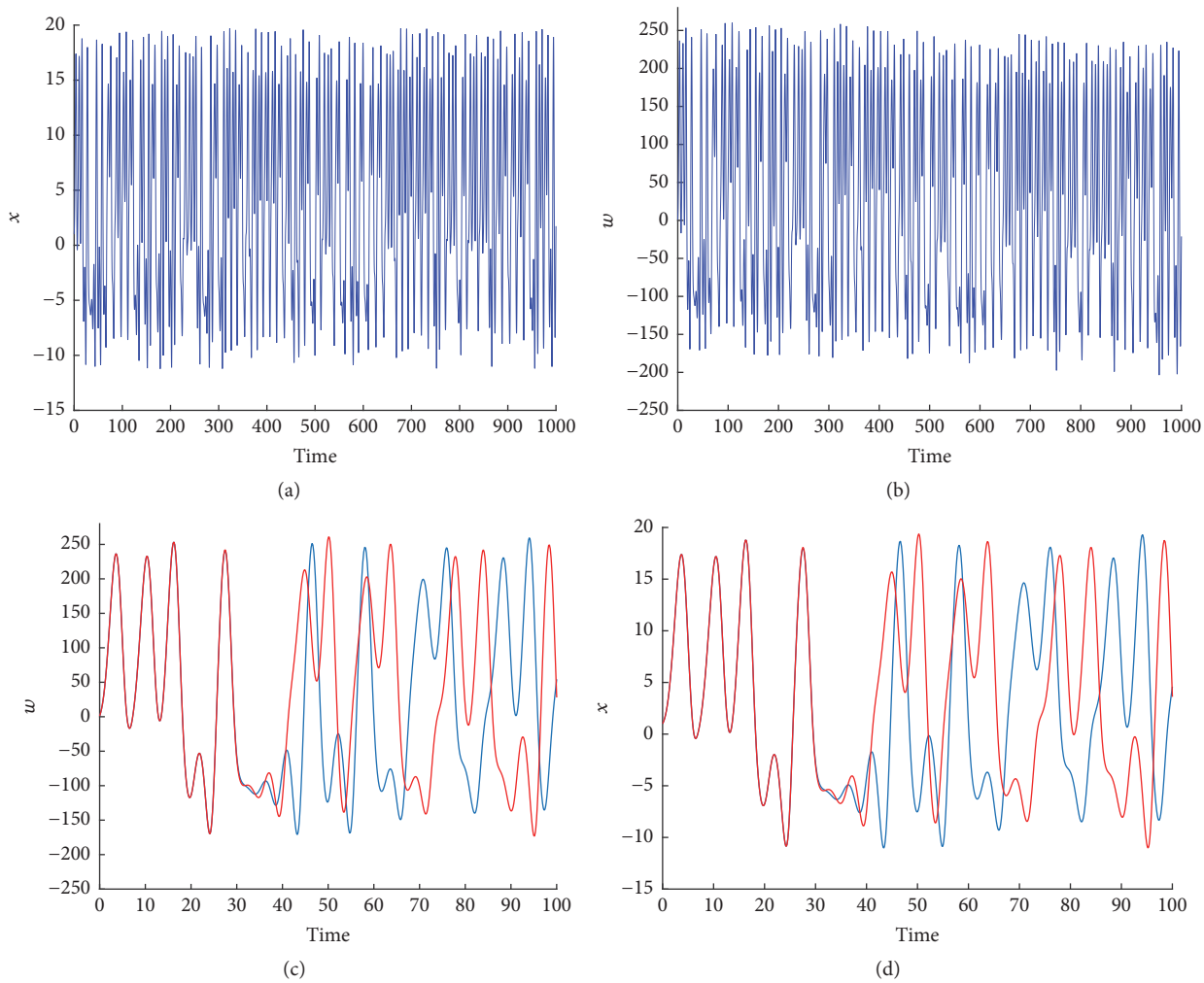

FIGURE 2: Time series and sensitive dependence on initial conditions (1, 1, 1, 1) (blue) and (1.001, 1, 1, 1) (red): (a) and (d) variable x; (b) and (c) variable w.

an asymmetrical form with respect to all the principal axes characterized by two scrolls of different sizes.

The time series of the state variables x and w are described in Figures 2(a) and 2(b). These signals represent the chaotification rates of each variable. On the other hand, system (1) is sensitive to initial conditions as shown in Figures 2(c) and 2(d). Note that the variation range of the variable w is extended within $[-250, 200]$, unlike the other variables. This point must be considered in practical applications.

3. Dynamic Analysis

3.1. Equilibrium and Stability. The equilibrium points of system (1) are obtained by solving these equations:

$$\begin{aligned} y = z = w = 0, \\ -cx^2 + d\,|x|\,x + m\,|x|^r\,x^{-1} = 0. \end{aligned} \tag{5}$$

Proposition 1. *(i) If $x = 0$, then $w = 0$ and the origin $H_1 = (0, 0, 0, 0)$ is the first equilibrium of system (1).*

(ii) If $x > 0$, then $w = 0$ and $H_2 = (((c-d)/m)^{1/\alpha}, 0, 0, 0)$ is an equilibrium of system (2) where $\alpha = r - 3$.

(iii) If $x < 0$, then $w = 0$ and $H_3 = ((-(-c-d)/m)^{1/\alpha}, 0, 0, 0)$ is an equilibrium of system (2) where $\alpha = r - 3$.

Proof. Case (i) is obvious.

For case (ii), we should solve the following equation: $-c + d + mx^{r-3} = 0$ which admits the solution $x^\alpha = (c-d)/m$ with $\alpha = r - 3$. The roots of this equation are given by [22]

$$x = \left|\frac{(c-d)}{m}\right|^{1/\alpha} e^{(j\theta_1 \pm 2n\Pi)/\alpha} \tag{6}$$

with $n \in \mathbb{N}$, θ_1 being the phase of x^α, and α being a fractional number. Notice that the term $(c-d)/m$ is positive when $c = -0.11$, $d = -0.21$, and $m = 6.26$. Then, θ_1 is equal to zero and we have $x = ((c-d)/m)^{1/\alpha}$.

For case (iii), we should solve the following equation: $-c - d - m(-x)^{r-3} = 0$ which admits the solution $(-x)^\alpha = X^\alpha = (-c-d)/m$ with $\alpha = r - 3$. The roots of this equation are given by [22]

$$X = \left|\frac{(-c-d)}{m}\right|^{1/\alpha} e^{(j\theta_2 \pm 2n\Pi)/\alpha} \tag{7}$$

Table 1: Stability analysis of system (1).

Equilibrium point	Jacobian matrix	Corresponding eigenvalues	Stability analysis
H_1	$\begin{pmatrix} 0 & 1 & 0 & 0 \\ 0 & 0 & 1 & 0 \\ 0 & -b & -a & 0 \\ 0 & k & 0 & -h \end{pmatrix}$	$\lambda_1 = 0$ $\lambda_2 = -0.001$ $\lambda_3 = -0.465 + 0.945i$ $\lambda_4 = -0.465 - 0.945i$	Stable point
H_2	$\begin{pmatrix} 0 & 1 & 0 & 0 \\ 0 & 0 & 1 & 0 \\ \Delta_1 & -b & -a & 0 \\ \Delta_1 & k & 0 & -h \end{pmatrix}$	$\lambda_1 = -0.001$ $\lambda_2 = -1.273$ $\lambda_3 = 0.171 + 1.232i$ $\lambda_4 = 0.171 - 1.232i$	Unstable point
$\Delta_1 = 2dx - 2cx + (r-1)mx^{r-2}$			
H_3	$\begin{pmatrix} 0 & 1 & 0 & 0 \\ 0 & 0 & 1 & 0 \\ \Delta_2 & -b & -a & 0 \\ \Delta_2 & k & 0 & -h \end{pmatrix}$	$\lambda_1 = -0.001$ $\lambda_2 = -2.297$ $\lambda_3 = 0.683 + 1.945i$ $\lambda_4 = 0.683 - 1.945i$	Unstable point
$\Delta_2 = -2dx - 2cx - (r-1)mx^{r-2}$			

with $n \in \mathbb{N}$, θ_2 being the phase of x^α, and α being a fractional number. Notice that the term $(-c-d)/m$ is positive when $c = -0.11$, $d = -0.21$, and $m = 6.26$. Then, θ_2 is equal to zero and we have $x = (-(-c-d)/m)^{1/\alpha}$.

When the parameters (a, b, c, d, m, r, h, k) are equal to $(0.93, 1.11, -0.11, -0.21, 6.26, 1.32, 0.001, 14)$, system (1) admits three equilibrium points: $H_1 = (0, 0, 0, 0)$, $H_2 = (11.73, 0, 0, 0)$, and $H_3 = (-5.87, 0, 0, 0)$. For the stability analysis, Table 1 gives the Jacobian matrix J and its corresponding eigenvalues calculated for each equilibrium point. □

3.2. Lyapunov Exponents Analysis. System (1) exhibits four Lyapunov exponents (LEs). These LEs are esteemed using the Wolf algorithm [23], as shown in Figure 3 as

$$\begin{aligned} \mathrm{LE}_1 &= 0.232, \\ \mathrm{LE}_2 &= 0.020, \\ \mathrm{LE}_3 &= 0, \\ \mathrm{LE}_4 &= -1.169. \end{aligned} \tag{8}$$

Since the LE spectrum has two positive Lyapunov exponents; thus system (1) is hyperchaotic. λ_1 is the largest positive one. This exponent increases the expansion degree of the attractor in the phase space.

In addition, the corresponding Kaplan-Yorke dimension is

$$D_L = 3 + \frac{(\lambda_1 + \lambda_2 + \lambda_3)}{|\lambda_4|} = 3.19. \tag{9}$$

3.3. Routes to Chaos. System (1) can display periodic orbits, chaos, and hyperchaos attractors under different conditions. In fact, when the parameter m varies and the parameters (a, b, c, d, r, h, k) are fixed, two Hopf bifurcations are detected as shown in Figure 4. These bifurcations are denoted H in the bifurcation diagram and they appear when $m = 0.99$ and $m = 2.11$, respectively. Each Hopf point is characterized by a

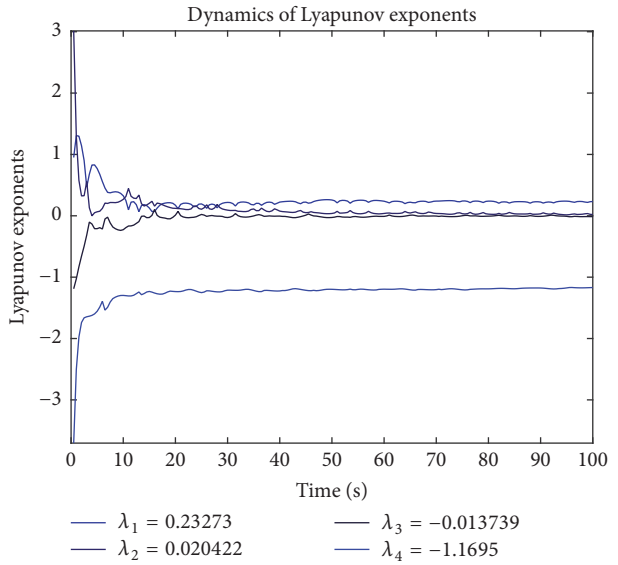

Figure 3: The Lyapunov exponent spectrum of the hyperchaotic system (1).

first Lyapunov coefficient (FLC). A positive FLC indicates the existence of a supercritical Hopf bifurcation, whereas a negative one indicates a subcritical Hopf bifurcation. In system (1), the two points obtained are supercritical Hopf bifurcations. This type of bifurcation indicates that the evolution to chaotic behavior is possible.

In addition, as the parameter of bifurcation m increases, system (1) undergoes the following routes:

(i) If $-1 \leq m \leq 0.3$, then system (1) exhibits periodic orbit. Figure 5(a) shows this regular attractor with $m = -0.5$.

(ii) If $0.3 < m \leq 2.1$, then system (1) converges to a fixed point as shown in Figure 5(b).

Table 2: The LEs of some typical attractors of system (1).

m	LE_1	LE_2	LE_3	LE_4	Attractor
3.6	0	0	−0.42	0.8	Periodic orbit
3.8	0.05	0	−0.01	−0.92	Chaotic attractor
6	0.18	0.007	0	−1.10	Hyperchaotic attractor
6.5	0.17	0.01	0	−1.16	Hyperchaotic attractor

Table 3: Comparative analysis with related hyperchaotic systems.

Hyperchaotic system	Lyapunov exponents	Kaplan-Yorke dimension
Proposed hyperchaotic system	$LE_1 = 0.231$ $LE_2 = 0.020$ $LE_3 = 0$ $LE_4 = -1.169$	$D_{KY} = 3.19$
Piecewise linear hyperchaotic circuit [25]	$LE_1 = 0.064$ $LE_2 = 0.033$ $LE_3 = 0$ $LE_4 = -1.098$	$D_{KY} = 3.089$
Hyperchaotic hyperjerk system [26]	$LE_1 = 0.142$ $LE_2 = 0.046$ $LE_3 = 0$ $LE_4 = -1.396$	$D_{KY} = 3.134$

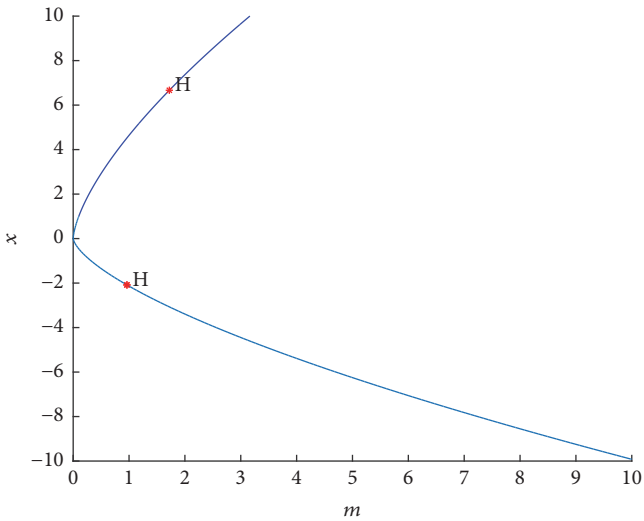

Figure 4: Hopf bifurcations.

(iii) If $2.1 < m \leq 3.8$, then another periodic orbit is obtained as shown in Figure 5(c) with $m = 1$.

(iv) If $3.8 < m \leq 5.5$, system (1) exhibits chaotic attractor. Figure 5(d) shows this strange attractor with $m = 4.5$.

(v) If $5.5 < m < 7$, then system (1) exhibits hyperchaotic attractor. Figure 5(e) shows this strange attractor with $m = 6$.

Some typical attractors are tabulated in Table 2 according to the parameter m.

3.4. Comparative Analysis. Referring to the survey paper [24], the first Lyapunov exponent can be one of the comparative criteria between hyperchaotic systems. Table 3 presents a comparative analysis between system (1) and two related ones, recently proposed in literature. Such a choice is based on the fact that, identical to system (1), the first comparative example contains linear piecewise functions whereas the second one is based on the jerk equation. Based on Table 3, it is clear that system (1) exhibits more complex dynamics. Thus, this confirms the highlight potential applications of noninteger order terms with respect to classical nonlinear terms.

4. Circuit Design

It is obvious that hardware implementation of chaotic systems is an interesting task in engineering applications, namely, for secure communications and random bits generation. Therefore, the aim of this section is to design an analog circuit that can build hyperchaotic behaviors according to system (1).

4.1. Design of the Analog Circuit with MultiSIM. For the circuit implementation, we choose the particular case study when the system parameter r is fixed to 1.5. Thus, the proposed system will be defined by the following model:

$$\begin{aligned} \dot{x} &= y, \\ \dot{y} &= z, \\ \dot{z} &= -az - by - cx^2 + d\,|x|\,x + m\sqrt{|x|}\,\mathrm{sgn}\,(x) \\ \dot{w} &= ky - hw - cx^2 + d\,|x|\,x + m\sqrt{|x|}\,\mathrm{sgn}\,(x), \end{aligned} \tag{10}$$

where the system parameters (a, b, c, d, m, h, k) are equal to $(1, 1, -0.11, -0.21, 5, 0.01, 14)$. System (10) exhibits four LEs such as

$$LE_1 = 0.18,$$
$$LE_2 = 0.04,$$

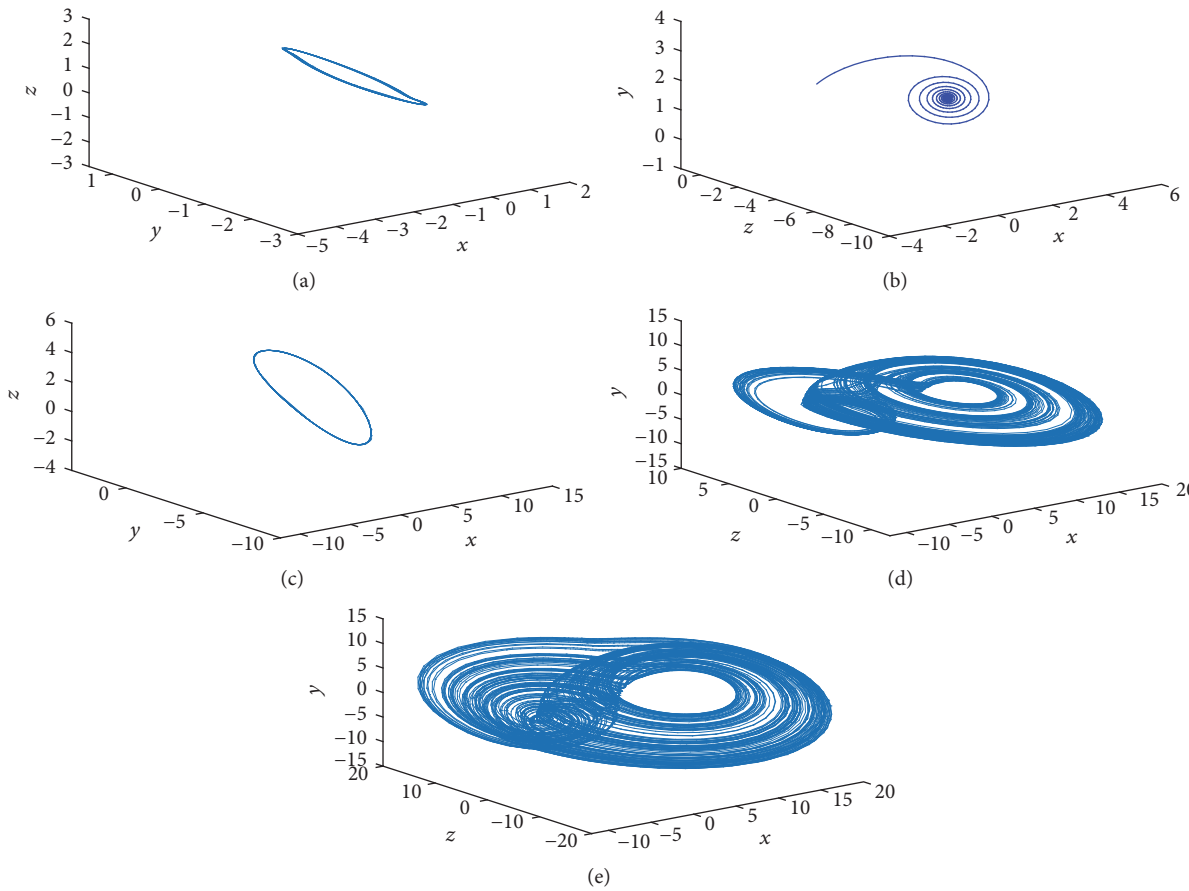

Figure 5: Different attractors forms exhibited by system (1) when parameter m varies.

$$\begin{aligned} \mathrm{LE}_3 &= 0, \\ \mathrm{LE}_4 &= -1.2. \end{aligned} \tag{11}$$

Despite the observation of the obtained phase portraits of system (10), we deduce that the maximum value of the signal w can reach the level of 250. Thus, 250 V is a sufficiently high voltage for the common components used in the proposed circuit. Therefore, a linear transformation for system (10) is necessary to decrease the amplitude of the state variables. Letting $u = x/2$, $v = y/2$, $g = z/2$, and $f = w/160$ and then setting the original state variables x, y, z, and w instead of the variable u, v, g, and f, the adjusted system becomes the following one:

$$\begin{aligned} \dot{x} &= y, \\ \dot{y} &= z, \\ \dot{z} &= az - by - 2cx^2 + 2d\,|x|\,x + \frac{m}{\sqrt{2}}\sqrt{|x|}\mathrm{sgn}\,(x) \\ \dot{w} &= ky - 80hw - 2cx^2 + 2d\,|x|\,x + \frac{m}{\sqrt{2}}\sqrt{|x|}\mathrm{sgn}\,(x)\,. \end{aligned} \tag{12}$$

The amplitude of the state variables of system (10) has decreased as shown in Figure 6. Moreover, the two systems (10) and (12) are equivalent since the linear transformation does not change the physical properties of nonlinear systems.

To design the hyperchaotic circuit of system (12), only common electronic components are used such as resistors, capacitors, diodes, multipliers, and operational amplifiers. In fact, the nonlinear terms of system (12) should be designed first, namely, the quadratic term, the absolute function, the sign function, and the square root function. The quadratic term is implemented with the analog multiplier. The square root element is designed with two operational amplifiers as only active elements [27]. The analog circuit of the square root element is provided in Figure 7.

For the theoretical study and based on [27], the second voltage source in Figure 7 should be fixed to 2.878 V. However, in experimentation applications, we have obtained the root square function by using a stabilized voltage equal to 2.9 V as shown in Figure 8. This figure describes two voltages; the first one is a positive source signal and the second one is the output signal of the square root circuit. Based on these results, the observed maximum voltages are equal to 720 mV and 900 mV ($\simeq \sqrt{0.72} = 0.88$), respectively. Thus, the square root function is correctly obtained with 2.9 V. In addition, based on MultiSIM results and experimental simulations, if the source voltage is included in [2.7 V, 3 V] then system (12) generates strange attractors. To avoid making this paper more cumbersome, details on experiments and experimental results will be soon presented in future works, confirming the MultiSIM results.

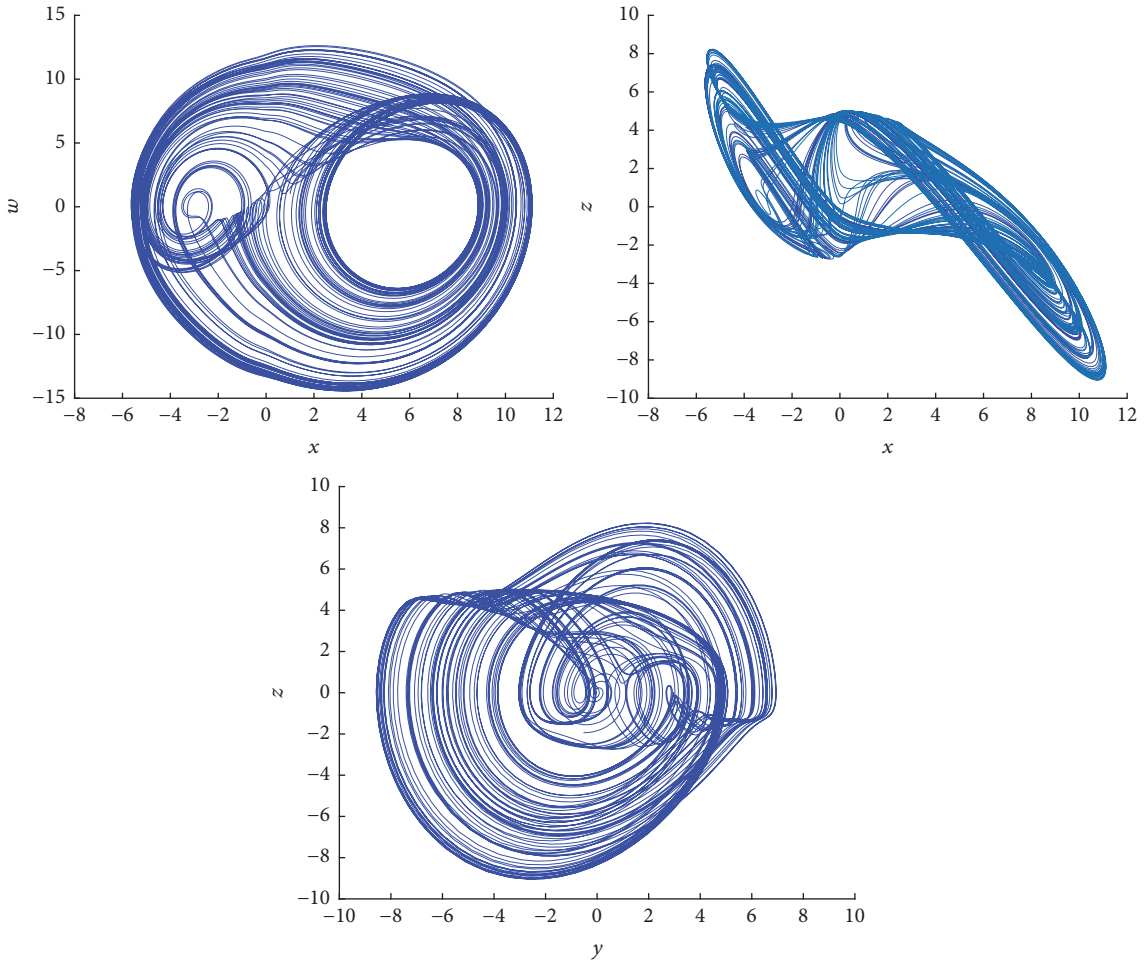

Figure 6: Projections of the attractor related to the adjusted hyperchaotic system (12) onto the spaces (x, w), (x, z), and (y, z).

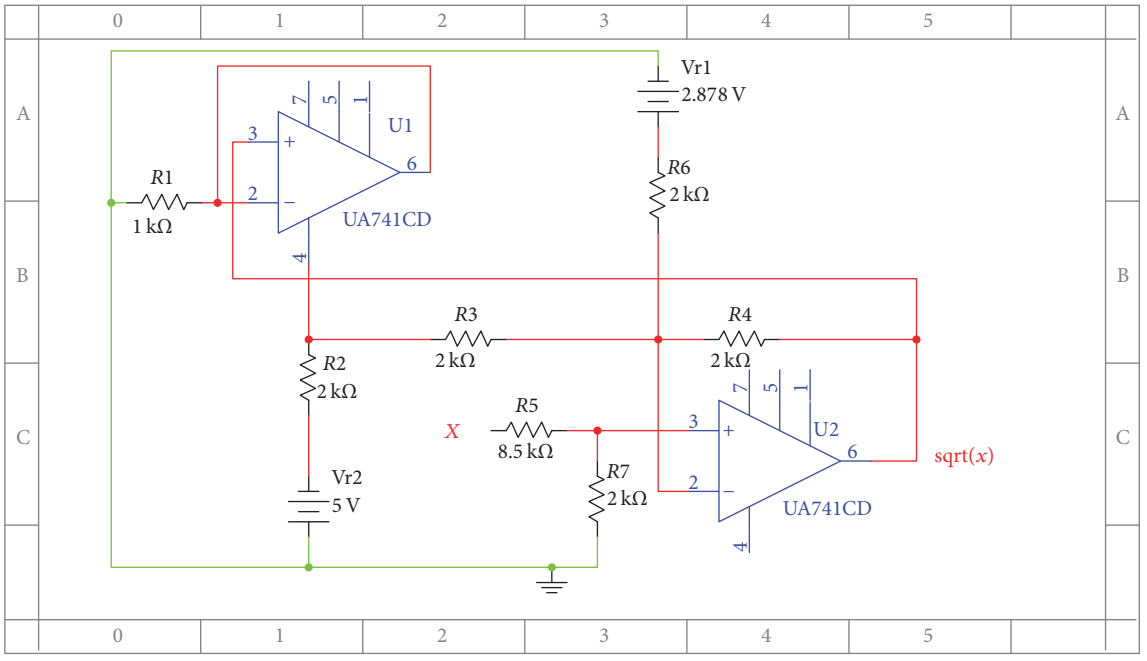

Figure 7: Circuit design of the square root function with MultiSIM.

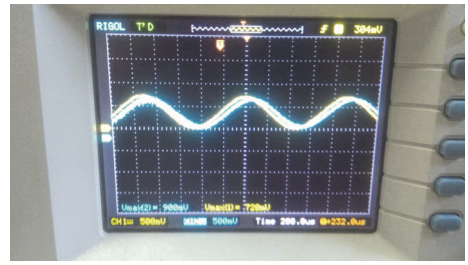

Figure 8: Experimental results of the square root function.

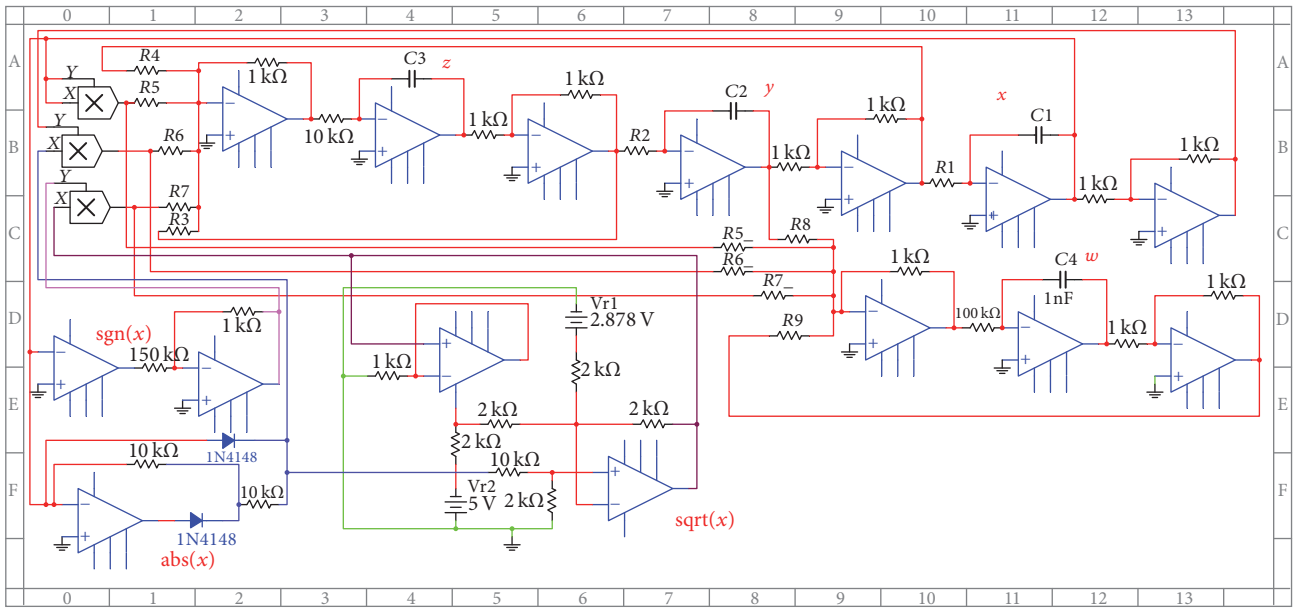

Figure 9: Circuit design of the hyperchaotic system with MultiSIM.

The corresponding circuit equation of the hyperchaotic system can be described as

$$\begin{aligned}
\dot{x} &= \frac{1}{R_1 C_1} y, \\
\dot{y} &= \frac{1}{R_2 C_2} z, \\
\dot{z} &= -\frac{1}{R_3 C_3} z - \frac{1}{R_4 C_3} y + \frac{1}{R_5 C_3} x^2 - \frac{1}{R_6 C_3} |x| x \\
&\quad + \frac{1}{R_7 C_3} \sqrt{|x|} \operatorname{sgn}(x) \\
\dot{w} &= -\frac{1}{R_8 C_4} y - \frac{1}{R_9 C_4} w + \frac{1}{R_5 C_4} x^2 - \frac{1}{R_6 C_4} |x| x \\
&\quad + \frac{1}{R_7 C_4} \sqrt{|x|} \operatorname{sgn}(x).
\end{aligned} \tag{13}$$

According to system (12) and (13) and design considerations, we fixed the values of the resistances and the capacitors as

$$\begin{aligned}
C_1 &= C_2 = C_3 = 1\,\text{nF}, \\
C_4 &= 0.1\,\text{nF}, \\
R_1 &= R_2 = 100\,\text{k}\Omega, \\
R_3 &= R_4 = 10\,\text{k}\Omega, \\
R_5 &= 4.554\,\text{k}\Omega, \\
R_6 &= 2.5\,\text{k}\Omega, \\
R_7 &= 0.2\,\text{k}\Omega, \\
R_8 &= 7\,\text{k}\Omega, \\
R_9 &= 1.25\,\text{k}\Omega.
\end{aligned} \tag{14}$$

Finally, the obtained circuit diagram, designed with Multi-SIM Software, is provided in Figure 9 where the multiplier is AD633 and the operator amplifier is UA741.

4.2. Simulation Results. For the oscillator circuit, all active devices (UA741 and AD633) are powered by ±15 V. Several design considerations were taken into account to prevent degrading the hyperchaotic behavior such as the adjustment of the resistors and the capacitors for the integration operations.

The oscilloscope traces of the proposed circuit are shown in Figure 10. Comparing the different hyperchaotic attractors shown in Figures 6 and 10, a good qualitative agreement

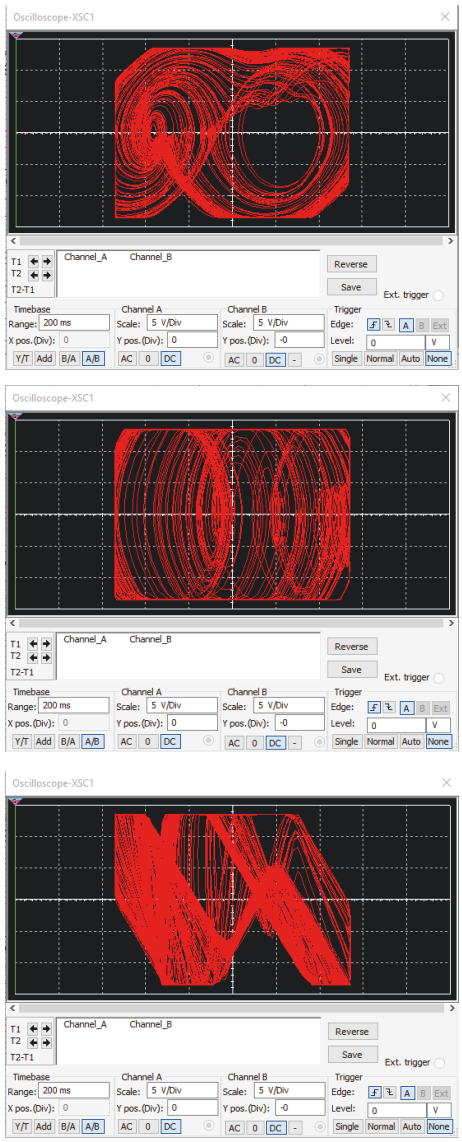

Figure 10: Simulation results of the hyperchaotic system with MultiSIM Software.

between the numerical simulations with Matlab and the electrical simulations with MultiSIM Software is observed. In fact, for MultiSIM Software, we have obtained the same attractors forms as those obtained by Matlab simulations. However, in these last attractors, some saturation effects are detected due to the operational amplifiers responses. To avoid making this paper more cumbersome, details on experiments and experimental results will be presented in future works, where saturation effects of amplifiers will be deeply analyzed.

5. Conclusions

In this paper, a novel hyperchaotic system is proposed by considering fractional-order polynomials. Analytical and numerical results show that this system exhibits more complex behaviors than those proposed by related works. Moreover, its analog circuit is designed and simulated with MultiSIM Software. In future works, experimental realization of the hyperchaotic circuit will be proposed and the saturation effects induced by the operational amplifiers will be analyzed. Thereafter, the proposed circuit will be considered for secure image encryption and decryption applications.

Conflicts of Interest

The authors declare that there are no conflicts of interest regarding the publication of this paper.

References

[1] O. E. Rossler, "An equation for hyperchaos," *Physics Letters A*, vol. 71, no. 2-3, pp. 155–157, 1979.

[2] T. Matsumoto, L. Chua, and K. Kobayashi, "Hyperchaos: laboratory experiment and numerical confirmation," *IEEE Transactions on Circuits and Systems*, vol. 33, no. 11, pp. 1143–1147, 1986.

[3] C.-L. Li, J.-B. Xiong, and W. Li, "A new hyperchaotic system and its generalized synchronization," *Optik-International Journal for Light and Electron Optics*, vol. 125, no. 1, pp. 575–579, 2014.

[4] Z. Wei, R. Wang, and A. Liu, "A new finding of the existence of hidden hyperchaotic attractors with no equilibria," *Mathematics and Computers in Simulation*, vol. 100, pp. 13–23, 2014.

[5] K. Rajagopal, L. Guessas, S. Vaidyanathan, A. Karthikeyan, and A. Srinivasan, "Dynamical analysis and FPGA implementation of a novel hyperchaotic system and its synchronization using adaptive sliding mode control and genetically optimized PID control," *Mathematical Problems in Engineering*, vol. 2017, Article ID 7307452, 14 pages, 2017.

[6] Y. Feng, Z. Wei, U. E. Kocamaz, A. Akgül, and I. Moroz, "Synchronization and electronic circuit application of hidden hyperchaos in a four-dimensional self-exciting homopolar disc dynamo without equilibria," *Complexity*, vol. 2017, Article ID 7101927, 11 pages, 2017.

[7] Z. Wei and W. Zhang, "Hidden hyperchaotic attractors in a modified lorenz-stenflo system with only one stable equilibrium," *International Journal of Bifurcation and Chaos*, vol. 24, no. 10, article 1450127, 2014.

[8] A. T. Azar, C. Volos, N. A. Gerodimos et al., "A novel chaotic system without equilibrium: Dynamics, synchronization, and circuit realization," *Complexity*, vol. 2017, Article ID 7871467, 11 pages, 2017.

[9] A. E. Matouk, "Chaos, feedback control and synchronization of a fractional-order modified autonomous Van der Pol-Duffing circuit," *Communications in Nonlinear Science and Numerical Simulation*, vol. 16, no. 2, pp. 975–986, 2011.

[10] M. Mamat, W. S. Mada Sanjaya, and D. S. Maulana, "Numerical simulation chaotic synchronization of Chua circuit and its application for secure communication," *Applied Mathematical Sciences*, vol. 7, no. 1-4, pp. 1–10, 2013.

[11] T. L. Carroll, "A simple circuit for demonstrating regular and synchronized chaos," *American Journal of Physics*, vol. 63, no. 4, pp. 377–379, 1995.

[12] J. C. Sprott, "Some simple chaotic flows," *Physical Review E: Statistical, Nonlinear, and Soft Matter Physics*, vol. 50, no. 2, part A, pp. R647–R650, 1994.

[13] H. P. Gottlieb, "What is the simplest jerk function that gives chaos?" *American Journal of Physics*, vol. 64, no. 5, article 525, 1996.

[14] J. C. Sprott, "A new class of chaotic circuit," *Physics Letters A*, vol. 266, no. 1, pp. 19–23, 2000.

[15] E. Campos-Cantón, "Chaotic attractors based on unstable dissipative systems via third-order differential equation," *International Journal of Modern Physics C*, vol. 27, no. 1, 2016.

[16] R. J. Escalante-González, E. Campos-Cantón, and M. Nicol, "Generation of multi-scroll attractors without equilibria via piecewise linear systems," *Chaos: An Interdisciplinary Journal of Nonlinear Science*, vol. 27, no. 5, article 053109, 2017.

[17] R. J. Escalante-González and E. Campos-Cantón, "Generation of chaotic attractors without equilibria via piecewise linear systems," *International Journal of Modern Physics C*, vol. 28, no. 1, article 1750008, 2017.

[18] V. Patidar and K. K. Sud, "Bifurcation and chaos in simple jerk dynamical systems," *Pramana—Journal of Physics*, vol. 64, no. 1, pp. 75–93, 2005.

[19] S. Vaidyanathan, C. Volos, V.-T. Pham, K. Madhavan, and B. A. Idowu, "Adaptive backstepping control, synchronization and circuit simulation of a 3-D novel jerk chaotic system with two hyperbolic sinusoidal nonlinearities," *Archives of Control Sciences*, vol. 24, no. 3, pp. 375–403, 2014.

[20] Z. Wei, V.-T. Pham, T. Kapitaniak, and Z. Wang, "Bifurcation analysis and circuit realization for multiple-delayed wangchen system with hidden chaotic attractors," *Nonlinear Dynamics*, vol. 85, no. 3, pp. 1635–1650, 2016.

[21] P. Li, T. Zheng, C. Li, X. Wang, and W. Hu, "A unique jerk system with hidden chaotic oscillation," *Nonlinear Dynamics*, vol. 86, no. 1, pp. 197–203, 2016.

[22] A. G. Radwan, A. M. Soliman, A. S. Elwakil, and A. Sedeek, "On the stability of linear systems with fractional-order elements," *Chaos, Solitons & Fractals*, vol. 40, no. 5, pp. 2317–2328, 2009.

[23] A. Wolf, J. B. Swift, H. L. Swinney, and J. A. Vastano, "Determining Lyapunov exponents from a time series," *Physica D: Nonlinear Phenomena*, vol. 16, no. 3, pp. 285–317, 1985.

[24] A. Lassoued and O. Boubaker, "On new chaotic and hyperchaotic systems: a literature survey," *Lithuanian Association of Nonlinear Analysts. Nonlinear Analysis: Modelling and Control*, vol. 21, no. 6, pp. 770–789, 2016.

[25] C. Li, J. C. Sprott, W. Thio, and H. Zhu, "A new piecewise linear hyperchaotic circuit," *IEEE Transactions on Circuits and Systems II: Express Briefs*, vol. 61, no. 12, pp. 977–981, 2014.

[26] S. Vaidyanathan, "Analysis, adaptive control and synchronization of a novel 4-D hyperchaotic hyperjerk system via backstepping control method," *Archives of Control Sciences*, vol. 26, no. 3, pp. 311–338, 2016.

[27] T. Kamsri, P. Julsereewong, and V. Riewruja, "Simple square-root extractor using op amps," in *Proceedings of the 2008 International Conference on Control, Automation and Systems, ICCAS 2008*, pp. 1812–1815, October 2008.